



Relative Hypoxia and Early Diabetic Kidney Disease in Type 1 Diabetes

Carissa Vinovskis,¹ Lu-Ping Li,² Pottumarthi Prasad,² Kalie Tommerdahl,¹ Laura Pyle,¹ Robert G. Nelson,³ Meda E. Pavkov,⁴ Daniel van Raalte,⁵ Marian Rewers,⁶ Marlon Pragnell,⁷ Farid H. Mahmud,⁸ David Z. Cherney,⁹ Richard J. Johnson,¹⁰ Kristen J. Nadeau,¹ and Petter Bjornstad^{1,10}

Diabetes 2020;69:2700–2708 | <https://doi.org/10.2337/db20-0457>

The objective of this study was to compare the ratio of renal oxygen availability (RO₂) to glomerular filtration rate (GFR), a measure of relative renal hypoxia, in adolescents with and without type 1 diabetes (T1D) and relate the ratio to albuminuria, renal plasma flow (RPF), fat mass, and insulin sensitivity (*M/I*). RO₂ was estimated by blood oxygen level–dependent MRI; fat mass was estimated by DXA; GFR and RPF were estimated by iohexol and *p*-aminohippurate clearance; albuminuria was estimated by urine albumin-to-creatinine ratio (UACR); and *M/I* was estimated from steady-state glucose infusion rate/insulin (mg/kg/min) by hyperglycemic clamp in 50 adolescents with T1D (age 16.1 ± 3.0 years, HbA_{1c} 8.6 ± 1.2%) and 20 control patients of similar BMI (age 16.1 ± 2.9 years, HbA_{1c} 5.2 ± 0.2%). The RO₂:GFR (mL/min) was calculated as RO₂ (T2*, ms) divided by GFR (mL/min). Whole-kidney RO₂:GFR was 25% lower in adolescents with T1D versus control patients (*P* < 0.0001). In adolescents with T1D, lower whole-kidney RO₂:GFR was associated with higher UACR (*r* = −0.31, *P* = 0.03), RPF (*r* = −0.52, *P* = 0.0009), and fat mass (*r* = −0.33, *P* = 0.02). Lower medullary RO₂:GFR was associated with lower *M/I* (*r* = 0.31, *P* = 0.03). In conclusion, adolescents with T1D exhibited relative renal

hypoxia that was associated with albuminuria and with increased RPF, fat mass, and insulin resistance. These data suggest a potential role of renal hypoxia in the development of diabetic kidney disease.

Almost 30% of people with type 1 diabetes (T1D) will develop diabetic kidney disease (DKD) (1). Current treatments, such as control of hyperglycemia and hypertension, are beneficial but only partially protect against DKD. Finding new, safe, and effective therapies to halt early DKD progression in patients with T1D has proven to be challenging as demonstrated by the outcomes from the recent Adolescent Type 1 Diabetes Cardio-Renal Intervention Trial (AddIT) of ACE inhibitors and the adult Preventing Early Renal Loss in Diabetes (PERL) trials of uric acid lowering (2,3). A potential explanation for the failure of these trial is the narrow focus on the easily detectable clinical manifestations of disease, such as hyperglycemia and hypertension, rather than identifying and targeting the deeper metabolic derangements driving DKD.

T1D is a complex metabolic disorder with pathophysiological disturbances beyond β-cell injury, now recognized

¹Section of Endocrinology, Department of Pediatrics, University of Colorado School of Medicine, Aurora, CO

²Department of Radiology, NorthShore University HealthSystem, Evanston, IL

³Chronic Kidney Disease Section, Phoenix Epidemiology and Clinical Research Branch, National Institute of Diabetes and Digestive and Kidney Diseases, Phoenix, AZ

⁴Division of Diabetes Translation, Centers for Disease Control and Prevention, Atlanta, GA

⁵Diabetes Center, Department of Internal Medicine, Amsterdam University Medical Centers, location VUmc, Amsterdam, the Netherlands

⁶Barbara Davis Center for Diabetes, University of Colorado School of Medicine, Aurora, CO

⁷JDRF, New York, NY

⁸Division of Endocrinology, Department of Pediatrics, University of Toronto School of Medicine, Toronto, Ontario, Canada

⁹Division of Nephrology, Department of Medicine, University of Toronto School of Medicine, Toronto, Ontario, Canada

¹⁰Division of Nephrology, Department of Medicine, University of Colorado School of Medicine, Aurora, CO

Corresponding author: Petter Bjornstad, petter.bjornstad@childrenscolorado.org

Received 1 May 2020 and accepted 27 July 2020

Clinical trial reg. nos. NCT03618420 and NCT03584217, clinicaltrials.gov

This article contains supplementary material online at <https://doi.org/10.2337/figshare.12728423>.

The findings and conclusions in this report are those of the authors and do not necessarily represent the official position of the Centers for Disease Control and Prevention.

© 2020 by the American Diabetes Association. Readers may use this article as long as the work is properly cited, the use is educational and not for profit, and the work is not altered. More information is available at <https://www.diabetesjournals.org/content/license>.

See accompanying article, p. 2578.

to include insulin resistance (IR), which is causally related to the development of DKD (4). The kidneys are highly metabolically active and are second only to the heart with respect to oxygen consumption per tissue mass. The high oxygen demand is necessary to maintain adequate ATP production for the Na^+/K^+ -ATPase (5). The principal determinants of renal ATP consumption are tubular sodium reabsorption and glomerular filtration rate (GFR). Emerging animal data suggest that the kidneys are unable to sufficiently compensate for the increased rate of ATP consumption in diabetes due to the effects of IR and mitochondrial dysfunction on substrate utilization (6,7). IR worsens during puberty, a time when the kidneys almost double in size, making adolescents particularly susceptible to hypoxia (8). Therefore, revealing the potential role of relative renal hypoxia, reflected by a mismatch between renal oxygen availability (RO_2) and renal energy expenditure in the kidneys of adolescents with T1D (Fig. 1), is critical to our understanding of the early mechanisms of diabetic kidney injury. Moreover, this information may inform the development of new therapeutics that could be administered while changes may still be reversible. Blood oxygen level-dependent (BOLD) MRI provides reliable and noninvasive quantification of RO_2 (9,10); however, to our knowledge, this has not been applied in young people with T1D. The objective of this study was to compare the ratio of RO_2 by BOLD MRI to iohexol-assessed GFR, a key determinant of renal energy expenditure, in adolescents with and without T1D and to correlate the RO_2 :GFR ratio with albuminuria, *p*-aminohippurate (PAH)-assessed renal plasma flow (RPF), fat mass, insulin sensitivity (*M/I*), and mitochondrial function. We hypothesized that adolescents with T1D have a lower RO_2 :GFR compared with healthy control patients and that a low RO_2 :GFR, which is a manifestation of relative renal hypoxia, is associated with elevated albuminuria, RPF, fat mass, and IR.

RESEARCH DESIGN AND METHODS

Study Design and Participants

Fifty adolescents with T1D (12–21 years of age, diabetes duration 1–10 years, and $\text{HbA}_{1c} < 11\%$) from the Copeptin in Adolescent Participants with Type 1 Diabetes and Early Renal Hemodynamic Function (CASPER) study (NCT03618420) and 20 healthy adolescent control patients (12–21 years of age) from the Renal Hemodynamics, Energetics and Insulin Resistance in Youth Onset Type 2 Diabetes Study (Renal-HEIR) (NCT03584217) were included in this analysis. Participants with T1D were recruited from the pediatric clinics at the Barbara Davis Center for Diabetes at the Anschutz Medical Campus, Aurora, Colorado. T1D was defined by the American Diabetes Association criteria plus the presence of GAD, islet cell, zinc transporter 8, and/or insulin autoantibodies and the need for exogenous insulin. Exclusion criteria are detailed in Supplementary Table 1. All participants were examined at our clinical research center, where tests were performed in the morning after a 12-h fast, preceded by 3 days of restricted physical

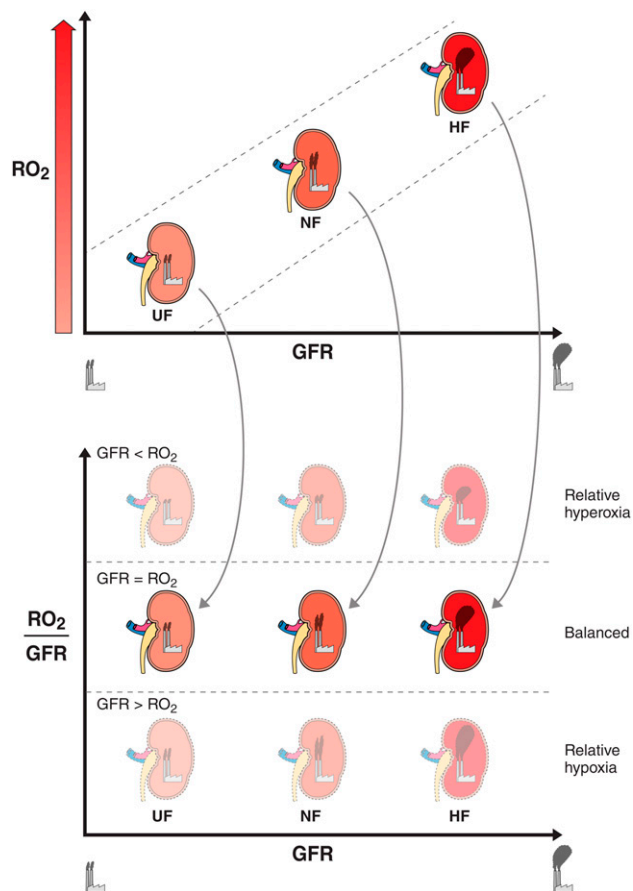


Figure 1— RO_2 :GFR and relative renal hypoxia. The top panel illustrates the relationship between RO_2 and GFR. A high GFR (workload) requires a high kidney oxygen availability to sustain the high energy expenditure. Therefore, whole-kidney hyperfiltration (HF) requires higher kidney oxygen availability compared with normofiltration (NF) and underfiltration (UF). The height of the smoke-stack plumes represents the magnitude of GFR. The bottom panel illustrates the ratio between RO_2 and GFR across UF, NF, and HF. Additionally, the bottom figure demonstrates three energetic scenarios across the stages of DKD: relative hyperoxia ($\text{RO}_2 > \text{GFR}$), balance ($\text{RO}_2 = \text{GFR}$), and relative hypoxia ($\text{RO}_2 < \text{GFR}$).

activity and a fixed-macronutrient, sodium, and protein replete, weight-maintenance diet. Participants remained fasted until after all study procedures were completed. The CASPER and Renal-HEIR cohorts have intentionally harmonized study protocols (see below) and were both approved by the Colorado Multiple Institutional Review Board. Participants or parents provided written informed assent and/or consent as appropriate for age.

GFR and RPF by Iohexol and PAH Clearance Techniques, Urine Albumin-to-Creatinine Ratio, and Blood Pressure

An intravenous (IV) line was placed, and participants were asked to empty their bladders. Spot plasma and urine samples were collected prior to iohexol and PAH infusion. Iohexol was administered through bolus IV injection (5 mL of 300 mg/mL; Omnipaque 300, GE Healthcare). An equilibration period of 120 min was used and blood

collections for iohexol plasma disappearance were drawn at +120, +150, +180, +210, +240 min (11). Because the Brøchner-Mortensen equation underestimates high values of GFR, the Jødal-Brøchner-Mortensen equation was used to calculate the GFR (12). PAH (2 g/10 mL, prepared at the University of Minnesota, with a dose of [weight in kg]/75 × 4.2 mL; IND #140129) was given slowly over 5 min followed by a continuous infusion of 8 mL of PAH and 42 mL of normal saline at a rate of 24 mL/h for 2 h. After an equilibration period, blood was drawn at 90 and 120 min, and RPF was calculated as PAH clearance divided by the estimated extraction ratio of PAH, which varies by the level of GFR (13). We report absolute GFR (mL/min) and RPF (mL/min) in the main analyses because the practice of indexing GFR and RPF for body surface underestimates hyperfiltration and hyperperfusion (14), and body surface area (BSA) calculations introduce noise into the clearance measurements. We also present GFR standardized by BSA in Table 1 for reference, and sensitivity analyses with RO_2 :GFR standardized by BSA in Supplementary Table 3.

In adolescents with T1D, GFR and RPF were measured during mild hyperglycemia (goal blood glucose 170–190 mg/dL [9.4–10.6 mmol/L]) achieved by a modified hyperglycemic clamp with paired 20% dextrose and insulin IV infusions, which were chosen to mimic the typical glycemic milieu of an adolescent with T1D (equivalent to HbA_{1c} ~7.6–8.2%) and maintain steady-state glycemic and insulin concentrations during renal measures (15,16). In control patients, GFR and RPF was measured fasting without glucose control to represent nondiabetic physiology. Urine albumin-to-creatinine ratio (UACR) was measured fasting from spot urine samples before and after renal clearance assessment and averaged.

Insulin Sensitivity (*M/I*) by Modified Hyperglycemic Clamp and Body Composition by DXA

M/I was calculated during the clamped hyperglycemia of the GFR and RPF measurements only in participants with T1D. A continuous infusion of 20% dextrose was titrated over 4 h, with a goal blood glucose of 170–190 mg/dL based on blood glucose measures taken every 5–10 min from the contralateral IV. Bedside blood glucose was measured by the StatStrip hospital-grade glucometer. A simultaneous insulin infusion was given to replace the exogenous insulin injections. Steady-state sampling of blood for glucose and insulin occurred at 240 min (*M/I* indicates the steady-state glucose infusion rate [GIR] in mg/kg fat-free mass [FFM]/min adjusted for steady-state insulin concentrations) during the same period was measured as in our previous hyperglycemic clamp studies (17,18).

Additionally, we calculated estimated insulin sensitivity (eIS) in all participants using a formula we previously validated against hyperinsulinemic-euglycemic clamps in participants with T1D and control patients, as $\text{exp}(4.64725 - 0.02032 [\text{waist circumference, cm}] - 0.09779 [\text{HbA}_{1c}, \%] - 0.00235 [\text{triglycerides, mg/dL}])$ (19). All participants also underwent DXA by standard methods on

Table 1—Baseline participant characteristics stratified by study

	T1D (n = 50)	Control (n = 20)	P value
Age (years)	16.0 ± 3.0	16.1 ± 2.9	0.94
Tanner stage	5 (4–5)	5 (4–5)	0.99
T1D duration (years)	5.7 ± 2.6	—	—
Sex, female (%)	50%	70%	0.13
Race/ethnicity (%)			
Black non-Hispanic	2	5	0.41
Hispanic	6	0	
White non-Hispanic	92	95	
Other	0	0	
BMI (kg/m ²)	23.4 ± 5.1	22.7 ± 3.7	0.58
Weight (kg)	67.5 ± 17.6	62.7 ± 14.5	0.28
Fat mass (kg)	20.3 ± 9.4	19.2 ± 6.7	0.62
Blood pressure (mmHg)			
Systolic blood pressure	119 ± 9	117 ± 8	0.30
Diastolic blood pressure	74 ± 11	73 ± 11	0.89
MAP	89 ± 9	88 ± 9	0.66
UACR (mg/g)	6 (5–14)	7 (4–10)	0.87
GFR (mL/min)	189 ± 40	136 ± 22	<0.0001
GFR (mL/min/1.73 m ²)	183 ± 26	139 ± 8	<0.0001
RPF (mL/min)	820 ± 125	615 ± 65	<0.0001
RPF (mL/min/1.73 m ²)	824 ± 120	634 ± 85	<0.0001
Hematocrit (%)	41.7 ± 2.8	41.8 ± 2.9	0.95
Lactate (mg/dL)	32.5 ± 7.2	27.9 ± 8.1	0.03
KIM-1 (pg/mL)	27.1 ± 12.4	28.4 ± 9.4	0.67
HbA _{1c} (%)	8.7 ± 1.3	5.2 ± 0.2	<0.0001
LDL cholesterol (mg/dL)	89 ± 24	92 ± 24	0.65
HDL cholesterol (mg/dL)	51 ± 10	46 ± 9	0.08
Triglycerides (mg/dL)	78 ± 35	88 ± 36	0.27
eIS	7.2 ± 2.1	9.9 ± 2.0	<0.0001
GIR at steady state (<i>M</i>) (mg/kg/min)	3.7 ± 1.9	—	—
Insulin at steady state (μIU/mL)	33 ± 18	—	—
<i>M/I</i> (mg/kg/min per μIU/mL insulin × 100)	10.9 (6.9–16.6)	—	—
<i>M/I</i> (mg/lean kg/min per μIU/mL insulin × 100)	15.7 (11.1–26.2)	—	—

Data are presented as mean ± SD or median (IQR), unless otherwise noted.

a Hologic device (Waltham, MA) to determine fat mass and FFM.

Laboratory Assessments

All laboratory assays for the CASPER and Renal-HEIR cohorts were performed by the University of Colorado Clinical Translational Research Center Core Laboratories and by the National Institute of Diabetes and Digestive and Kidney Diseases (NIDDK) laboratory. Insulin was measured via

Clinical Laboratory Improvement Amendments–certified chemiluminescent immunoassay (Beckman Coulter). Iohexol and PAH concentrations were measured in Phoenix by high-performance liquid chromatography (Waters, Milford, MA). Other fasting laboratory evaluations included the following: total cholesterol, LDL cholesterol, HDL cholesterol, triglycerides, glucose, and HbA_{1c} (Diabetes Control and Complications Trial-calibrated); assays were performed by standard methods in the Clinical Translational Research Center laboratory. Plasma kidney injury molecule 1 (KIM-1) was measured using the Meso Scale Discovery QuickPlex SQ120 platform (Meso Scale Diagnostics, Gaithersburg, MD). The Meso Scale assay is a sandwich immunoassay organized in a patterned array format and uses electrochemiluminescence detection. KIM-1 was measured using the Meso Scale Discovery R-plex assays.

RO₂ and Furosemide-Suppressible O₂ Consumption by BOLD MRI

We performed BOLD sequences on a Skyra Siemens T3 scanner at our Research Imaging Center in all participants to quantify fractional oxygen availability (apparent relaxation rate [R2*], s⁻¹) and RO₂ (T2* = 1/R2*) (20). A multiple gradient-recalled echo sequence was used to acquire BOLD images in the coronal plane during breath-hold at end-expiration, before and after giving the diuretic furosemide (20 mg IV injection). MRI acquisition parameters for the multiple gradient-recalled echo sequences are listed in Supplementary Table 2. The body coil was used as the transmitter, and the combination of spine and body array coils was used as the receiver. For participants with T1D on insulin pumps, these devices were temporarily suspended and removed during MRI scanning as they were not MRI compatible. Blood glucose concentrations were recorded prior to and after the MRI scan. Participants were placed feet first in a supine position. The higher the local deoxyhemoglobin in the blood, the higher the R2* (lower T2*), and the lower the local tissue oxygen content. The RO₂:GFR (ms/mL/min), as a measure of relative renal hypoxia, was calculated as RO₂ (T2*, ms) divided by GFR (mL/min). BOLD MRI was obtained before and after a 20 mg injection of furosemide (9,21) (Supplementary Fig. 1). The change in fractional RO₂ (R2*) in response to furosemide provides an estimate of the oxygen-dependent tubular transport of sodium and renal oxygen consumption, entitled furosemide-suppressible O₂ consumption (FSOC) (Supplementary Fig. 1). The images were analyzed by an author (P.P.) at a laboratory at the Department of Radiology, NorthShore University HealthSystem, and the reader was blinded to the participants' clinical data.

Statistical Analysis

Means and SDs were calculated for continuous variables, except those with highly skewed distributions, which were summarized by medians and interquartile ranges (IQRs). Categorical variables were described with numbers and percentages. Baseline comparisons between adolescents

with T1D and control patients were accomplished by *t* tests and χ^2 tests as appropriate. For categorical measures with limited number of observations, Fisher's exact test was used. For continuous variables without normal distribution, the Wilcoxon rank-sum test was used. Pearson correlation coefficient and generalized linear regression models were used to examine the relationships between RO₂:GFR, RPF, albuminuria, blood pressure, HbA_{1c}, diabetes duration, lactate, hematocrit, KIM-1, M/I, eIS, and fat mass. Multivariable models were adjusted for age, sex, and HbA_{1c}. Age is an important determinant of kidney growth and size, and early DKD is characterized by sexual dimorphism. HbA_{1c} is a traditional risk factor for early DKD. In the multivariable models examining the relationships with FSOC, we also adjusted for weight to account for potential weight differences since furosemide 20 mg was administered to all participants. Data are considered hypothesis generating, a decision made a priori, and corrections for multiple comparisons were not performed. An α -value of 0.05 was considered statistically significant. All statistical analyses were performed in SAS, version 9.4 (SAS Institute Inc.).

Data and Resource Availability

The data sets generated and analyzed during this study, in addition to MRI, GFR, RPF, and modified hyperglycemic clamp protocols are available from the corresponding author upon reasonable request.

RESULTS

Participant Characteristics Stratified by T1D Status

Adolescents with and without T1D were similar in age, pubertal stage, ethnicity, BMI, fat mass, blood pressure, and lipids (Table 1). There were proportionally more girls without T1D, although this proportion was not statistically significant between the groups. As expected, participants with T1D had higher HbA_{1c}. T1D participants also had higher GFR and RPF consistent with hyperfiltration. Hematocrit and KIM-1 were similar in the two groups, whereas lactate, an indicator of tissue hypoxia, was higher in adolescents with T1D (Table 1).

RO₂:GFR and Renal O₂ Consumption in Adolescents With T1D and Control Patients

Whole-kidney RO₂:GFR, cortex RO₂:GFR, and medullary RO₂:GFR were 25%, 17%, and 22%, respectively, lower in participants with T1D compared with healthy control patients ($P < 0.0001$ for all) (Table 2). The differences remained statistically significant in multivariable models adjusted for sex and HbA_{1c}. Supplementary Table 3 shows sensitivity analyses with RO₂:GFR normalized by BSA, and the magnitude of differences between adolescents with and without T1D are similar and significant. Changes in whole-kidney and medullary oxygen availability in response to furosemide (FSOC) were numerically higher in participants with T1D compared with healthy control patients, suggesting higher oxygen consumption, but these differences did not reach statistical significance. In

Table 2—RO₂:GFR stratified by T1D status

	T1D (n = 50)	Control (n = 20)	P value	Adjusted P value†
RO ₂ :GFR by whole kidney, cortex, and medulla				
Whole-kidney RO ₂ :GFR (ms/mL/min)	0.24 ± 0.04	0.32 ± 0.04	<0.0001	0.0004
Cortex RO ₂ :GFR (ms/mL/min)	0.27 ± 0.05	0.36 ± 0.05	<0.0001	0.003
Medullary RO ₂ :GFR (ms/mL/min)	0.21 ± 0.04	0.27 ± 0.05	<0.0001	0.008
FSOC by whole kidney, cortex, and medulla				
Whole-kidney FSOC (ΔR2*)	3.06 ± 1.26	2.77 ± 0.95	0.36	0.03
Cortex FSOC (ΔR2*)	1.35 ± 1.15	1.53 ± 1.48	0.61	0.57
Medullary FSOC (ΔR2*)	6.37 ± 2.60	5.73 ± 1.87	0.34	0.48

Data are presented as mean ± SD. †Data are adjusted for sex and HbA_{1c} for RO₂:GFR, and sex, HbA_{1c}, GFR, for FSOC.

multivariable models, whole-kidney FSOC was higher in participants with T1D versus control patients (Table 2).

M/I in Adolescents With T1D and Control Patients

The eIS was lower in adolescents with T1D compared with control patients ($P < 0.0001$) (Table 1). The median blood glucose concentration during the modified hyperglycemic clamp in T1D participants was 183 (IQR 173–190) mg/dL and was similar to the median morning fasting blood glucose concentrations 177 (IQR 137–217) mg/dL. At steady state, the median insulin concentration was 31 (IQR 20–43) μ IU/mL, and GIR (M) was 3.4 (2.0–4.9) mg/kg/min or 5.2 (3.9–6.4) mg/kg FFM/min, providing a median M/I (per kg) of 10.9 (6.9–16.6) mg/kg/min per μ IU/mL insulin \times 100 or M/I (per FFM kg) of 15.7 (11.1–26.2) mg/kg FFM/min per μ IU/mL insulin \times 100.

Relationships Between RPF, Albuminuria, Blood Pressure, Lactate, Hematocrit, KIM-1, and RO₂:GFR in Adolescents With T1D

Higher RPF correlated strongly with lower whole-kidney RO₂:GFR ($r = -0.52$, $P = 0.009$), cortex RO₂:GFR ($r = -0.45$, $P = 0.005$), and medullary RO₂:GFR ($r = -0.62$, $P < 0.0001$), and these relationships remained significant in the multivariable models (Table 3). In the adjusted models, higher UACR and mean arterial pressure (MAP) correlated with lower whole-kidney RO₂:GFR (Table 3). Only six participants with T1D had elevated UACR (≥ 30 mg/g); thus, we examined RO₂:GFR across tertiles of UACR, and we found that participants in the highest UACR tertile had lower whole-kidney, cortex, and medullary RO₂:GFR compared with those in the lowest tertile after adjusting for age, sex, and HbA_{1c} (Fig. 2). Similar differences in RO₂:GFR were found across UACR tertiles when adjusting for diabetes duration, sex, and HbA_{1c} (data not shown). Higher serum lactate and hematocrit were also associated with lower whole-kidney and medullary RO₂:GFR (Table 3). Higher plasma KIM-1 also related to lower whole-kidney, cortex, and medullary RO₂:GFR in adjusted models (Table 3).

Relationships Among Adiposity, M/I, HbA_{1c}, and Diabetes Duration and RO₂:GFR in Adolescents With T1D

Fat mass and waist circumference correlated with lower whole-kidney, cortex, and medullary RO₂:GFR (Table 3).

Additionally, higher eIS and M/I correlated with higher medullary RO₂:GFR. In contrast, HbA_{1c} and diabetes duration did not correlate with RO₂:GFR (Table 3).

Determinants of Renal O₂ Consumption in Adolescents With T1D

In a multivariable model adjusting for age, sex, HbA_{1c}, and weight, whole-kidney RO₂:GFR inversely associated with whole-kidney FSOC ($\beta \pm$ SE: -7.1 ± 4.4 , $P = 0.12$), cortex RO₂:GFR inversely associated with cortex FSOC ($\beta \pm$ SE: -10.4 ± 3.2 , $P = 0.002$) and medullary RO₂:GFR inversely associated with medullary FSOC ($\beta \pm$ SE: -21.8 ± 10.4 , $P = 0.04$) in adolescents with T1D. These data reveal higher renal oxygen consumption in adolescents with T1D than healthy control patients and demonstrate a strong association between the higher renal oxygen consumption and relative renal hypoxia as assessed by a lower RO₂:GFR.

DISCUSSION

Renal hypoxia, stemming from a potential metabolic mismatch between increased renal energy expenditure and impaired substrate utilization, is increasingly proposed as a unifying early pathway in the development of DKD and a promising therapeutic target (6,7). In the current study, we demonstrate for the first time that adolescents with T1D had greater relative renal hypoxia, manifested as lower RO₂:GFR than healthy control patients, and the degree of relative renal hypoxia correlated with albuminuria within the normal range, blood pressure, lactate, hematocrit, and KIM-1, as well as adiposity and IR. Additionally, lower RO₂:GFR associated with higher renal oxygen consumption. Taken together, these data implicate renal hypoxia as an underlying mechanism of early diabetic kidney injury and support the hypothesis that the relative renal hypoxia may stem from increased energy expenditure due to elevated GFR (i.e., hyperfiltration) and impaired substrate metabolism due to IR.

Elevated GFR is prevalent in T1D and increases the filtered Na⁺ load which exacerbates the work of tubular Na⁺ reabsorption (22). Glucosuria also leads to increased Na⁺ transport by sodium–glucose cotransporter (SGLT) 1 and SGLT2 activity (23). Emerging animal data show that the kidneys are unable to compensate for the increased ATP consumption due to the effects of diabetes on fuel

Table 3—Determinants of RO₂:GFR in adolescents with T1D

Variables	Whole-kidney RO ₂ :GFR (ms/mL/min)			Cortex RO ₂ :GFR (ms/mL/min)			Medullary RO ₂ :GFR (ms/mL/min)		
	Crude values		Adjusted P value ^a	Crude values		Adjusted P value ^a	Crude values		Adjusted P value ^a
	r	P value		r	P value		r	P value	
RPF (mL/min)	−0.52	0.0009	0.004	−0.45	0.005	0.01	−0.62	<0.0001	0.003
Log UACR (mg/g)	−0.31	0.03	0.01	−0.26	0.07	0.04	0.24	0.10	0.06
MAP (mmHg)	−0.35	0.02	0.06	−0.29	0.04	0.048	−0.39	0.005	0.01
Heart rate (bpm)	0.10	0.51	0.69	0.07	0.65	0.70	0.12	0.42	0.51
Hematocrit (%)	−0.33	0.02	0.11	−0.27	0.06	0.11	−0.37	0.009	0.048
Lactate (mg/dL)	−0.34	0.02	0.004	−0.38	0.007	0.0009	−0.35	0.01	0.002
KIM-1 (pg/mL)	−0.27	0.06	0.04	−0.26	0.07	0.04	−0.26	0.07	0.047
Fat mass by DXA (kg)	−0.33	0.02	0.01	−0.29	0.049	0.02	−0.34	0.02	0.003
Waist circumference (cm)	−0.35	0.01	0.03	−0.28	0.05	0.07	−0.39	0.006	0.01
Length of diabetes (years)	−0.14	0.33	0.58	−0.19	0.19	0.33	−0.10	0.51	0.87
HbA _{1c} (%)	0.04	0.79	0.98	−0.07	0.61	0.51	−0.04	0.77	0.54
M// (per kg)	0.18	0.23	0.22	0.22	0.14	0.13	0.31	0.03	0.02
M// (per FFM)	0.15	0.33	0.37	0.19	0.20	0.22	0.29	0.049	0.054
eIS	0.30	0.04	0.13 ^b	0.27	0.07	0.09 ^b	0.39	0.006	0.03 ^b

^aAdjusted for age, sex, and HbA_{1c}. ^bAdjusted for age and sex, as HbA_{1c} is part of eIS equation.

generation (6,7). The less oxygen-efficient fuel profile in T1D is now thought to be secondary to IR that shifts renal fuel utilization toward free fatty acid oxidation (24,25), which has a lower ATP yield per oxygen consumed compared with other substrates (26,27). The net effect of the mismatch between increased ATP consumption and decreased ATP generation is increased renal oxygen consumption and the emergence of renal hypoxia, which may ultimately lead to functional impairment and progressive tissue injury. In fact, in experimental animal models of DKD, renal oxygen consumption is increased by up to 160% (28,29) and the increased renal oxygen consumption is strongly associated with renal hypoxia (30).

Oxygen quantification by BOLD MRI is limited to whole-kidney, cortex, and medulla and does not have the resolution to determine single-nephron oxygenation. Therefore, heterogeneity in oxygenation across renal subcompartments cannot currently be meaningfully measured with BOLD MRI. RO₂ by BOLD MRI is a function of nephron mass, renal perfusion and tissue O₂ consumption. The latter is determined by the balance between renal energy expenditure and substrate metabolism. Accordingly, to meaningfully examine early changes in RO₂, it is important to normalize RO₂ to nephron mass or workload (GFR). Since GFR is one of the principal determinants of RO₂ by BOLD MRI (31–33), the RO₂:GFR ratio provides a measure of relative renal hypoxia in young people with T1D (Fig. 1).

The imbalance between RO₂ and GFR in our study may reflect increased renal oxygen consumption considering the elevated workload (hyperfiltration) but also impaired substrate metabolism. Indeed, lower RO₂:GFR correlated with adiposity and measures of IR. The relationship with adiposity is also consistent with our previous data showing

strong relationships between measures of fat mass and renal hemodynamic dysfunction in T1D (34). Lower RO₂:GFR also correlated with higher plasma KIM-1, which has been linked with tubulointerstitial lesions, and chronic KIM-1 expression has been implicated in inflammation and tubulointerstitial fibrosis in experimental models (35). This observation suggests that chronic relative renal hypoxia in T1D may induce tubulointerstitial fibrosis, although a longitudinal study is needed to confirm this hypothesis. Glycemic control and diabetes duration did not associate with relative renal hypoxia in our study. The reason we did not find a significant association with diabetes duration may relate to our participant's short diabetes duration (only 5.7 ± 2.6 years). Consistent with our previous studies, IR was more strongly associated with early DKD than HbA_{1c} in adolescents with diabetes (36,37). Pubertal adolescents with T1D are known to have a greater degree of IR compared with prepubertal children and adults with T1D, likely related to increased growth hormone secretion (38,39). IR shifts renal fuel utilization toward free fatty acid oxidation (24,25), which has a lower ATP yield per oxygen consumed compared with other substrates (26,27). This shift in substrate metabolism therefore likely increases renal oxygen consumption as free fatty acid oxidation consumes more oxygen than other substrates. The Joslin Kidney Study demonstrated that early progressive renal decline (annual GFR decline ≥3.5 mL/min) is an early phenotype of DKD that may precede microalbuminuria (40), and we found that IR is an important risk factor for this phenotype in T1D (4). Therefore, it is plausible that early progressive renal decline may be characterized by progressive renal hypoxia. Future longitudinal studies are needed to quantify the

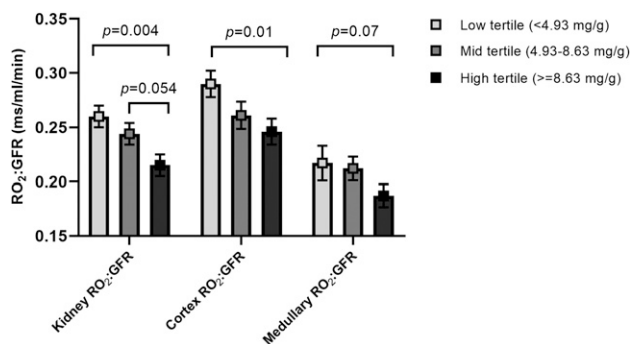


Figure 2—RO₂:GFR across tertiles of UACR. Kidney RO₂:GFR, cortex RO₂:GFR, and medullary RO₂:GFR across tertiles of UACR. Data presented are adjusted means (least square means) and SEs. Models are adjusted for age, sex, and HbA_{1c}.

relative renal hypoxia in individuals with progressive and stable GFR decline.

The metabolic mismatch may also shed light on potential nephroprotective mechanisms of novel adjunctive therapies in T1D, including SGLT2 inhibitors. SGLT2 inhibition has been shown to impede progression of DKD in large type 2 diabetes trials (41). Yet, the mechanisms of nephroprotection with SGLT2 inhibitors are poorly understood, and the salutary effects of this drug class are only partially mediated by the modest improvements in blood pressure, glycemic control, body weight, and serum urate. Although, there are no dedicated renal outcome trials with SGLT2 inhibitors in T1D, we have reported attenuated albuminuria (42) and hyperfiltration (16), major determinants of renal energy expenditure, in adults with T1D in response to SGLT2 inhibition. Computational rat kidney models also strongly support the role of attenuated renal oxygen consumption as a major nephroprotective effect of SGLT2 inhibitors (43). Additionally, SGLT2 inhibitors may improve IR (44) and support mitochondrial biogenesis (45). Correction of perturbed renal energetics are potential underlying mechanisms of SGLT2 inhibition in people with diabetes, and studies evaluating the effects of SGLT2 inhibitors on relative renal hypoxia in diabetes are needed.

To our knowledge this is the first study using BOLD MRI to quantify relative renal hypoxia in people with T1D. Additionally, the majority of renal BOLD MRI studies have been limited by the use of estimated GFR in lieu of gold standard measurements of GFR, and by the lack of detailed assessments of insulin sensitivity and adiposity (31–33). Our current study took advantage of directly measured GFR and RPF, assessed in T1D and non-T1D cohorts, innovations in imaging techniques to define changes in RO₂, and comprehensive metabolic phenotyping to define the earliest alterations in renal energetics that may contribute to the development of DKD in youth with T1D. Additionally, insulin sensitivity was assessed by calculating the *M/I* during a modified hyperglycemic clamp in addition to eIS. Our estimate of renal oxygen consumption by BOLD

MRI is based on IV administration of furosemide to examine changes in oxygen content as a result of suppressing oxygen consumption related to medullary tubular solute transport. Methods to quantify aerobic respiration more directly, including determining acetate-turnover in the Krebs cycle by ¹¹C-acetate positron emission tomography/computed tomography are likely superior to FSOC by BOLD but are less suitable in studies with pediatric participants due to the radiation exposure. The gold standard method to quantify *M/I* is by a hyperinsulinemic-euglycemic clamp, but since we wanted to assess GFR and RPF in adolescents with T1D during their typical glycemic milieu while maintaining steady-state glycemic and insulin concentrations during renal measures, we opted for a modified hyperglycemic clamp. Additionally, we wanted the fasting glycemic conditions during the BOLD MRI to match those during the renal clearance measurements. *M/I* by hyperglycemic clamp has shown to correlate strongly with *M/I* from gold-standard hyperinsulinemic-euglycemic clamps (46). By design, our study enrolled adolescents with short standing T1D (<10 years) to examine perturbed kidney energetics in the earliest stages of DKD (hyperfiltration). Consequently, our study findings may not be generalizable to adolescents with longstanding T1D or more advanced stages of DKD. Additionally, the relationships we observed between IR and relative renal hypoxia in our pubertal adolescents may not hold true in prepubertal children or adults with T1D who are more insulin sensitive. Another limitation is that UACR was measured by two repeated spot urine samples rather than three, which is the gold standard due to its variability. Moreover, the UACR correlates with GFR in early DKD, and this relationship may have confounded our RO₂:GFR results. Our kidney MRI protocol did not include dedicated sequences to accurately quantify total kidney volume, which may have been an important confounder in our analyses. Other limitations include the cross-sectional study design limiting causal inferences and the relatively small control group.

In conclusion, adolescents with T1D exhibit relative renal hypoxia that was associated with albuminuria within the normal range, elevated blood pressure, adiposity, and IR. These data suggest a role of perturbed renal energetics in the earliest stages of DKD. Future directions include examining the associations between RO₂:GFR trajectories and the progression of DKD, evaluation of early renal tissue injury, and perturbations of tissue-level expression on kidney biopsy as well as determining whether novel adjunctive therapies, including SGLT2 inhibitors, confer nephroprotection by attenuating renal hypoxia.

Funding. Financial support for this work was provided by the National Institute of Diabetes and Digestive and Kidney Diseases (NIDDK) Diabetic Complications Consortium (RRID:SCR_001415, www.diacomp.org), grants DK-076169 and DK115255 (18AU3871 [P.B.]), JDRF International grant 2-SRA-2018-627-M-B (P.B.), and National Institutes of Health NIDDK grant K23-DK-116720 (P.B.), National Heart, Lung, and Blood Institute grant K24-HL145076 (K.J.N.), and UL1-RR025780 (University of Colorado Denver), support from the Center for

Women's Health Research at University of Colorado, the Department of Pediatrics, Section of Endocrinology and Barbara Davis Center for Diabetes at University of Colorado School of Medicine, and by the Intramural Research Program of the NIDDK.

Duality of Interest. P.B. has consulted for AstraZeneca, Bayer, Bristol-Myers Squibb, Boehringer Ingelheim, Sanofi, Novo Nordisk, and Horizon Pharma and serves on the advisory boards of XORTX Therapeutics and Boehringer Ingelheim. No other potential conflicts of interest relevant to this article were reported.

Author Contributions. C.V. and P.B. wrote the manuscript and researched data. L.-P.L. assisted with MRI postprocessing and analyses. P.P. and L.P. developed the MRI protocols, postprocessing, and analyses. K.T. contributed to discussion and reviewed and edited the manuscript. L.P. was responsible for data analyses, contributed to the discussion, and reviewed and edited the manuscript. R.G.N. and his laboratory measured the iohexol and PAH concentrations, contributed to the discussion, and reviewed and edited the manuscript. M.E.P., D.v.R., M.P., and F.H.M. contributed to discussion and reviewed and edited the manuscript. M.R., D.Z.C., R.J.J., and K.J.N. assisted in study design, contributed to the discussion, and reviewed and edited the manuscript. P.B. designed the study. L.P. and P.B. are the guarantors of this work and, as such, had full access to all the data in the study and take responsibility for the integrity of the data and the accuracy of the data analysis.

Prior Presentation. Parts of this study were presented as an oral presentation at the 80th Scientific Sessions of the American Diabetes Association, 12–16 June 2020.

References

1. Reutens AT. Epidemiology of diabetic kidney disease. *Med Clin North Am* 2013;97:1–18
2. Marcovecchio ML, Chiesa ST, Bond S, et al.; AdDIT Study Group. ACE inhibitors and statins in adolescents with type 1 diabetes. *N Engl J Med* 2017;377:1733–1745
3. Doria A, Galecki A, Spino C, et al.; PERL Study Group Collaborators. Serum urate lowering with allopurinol and kidney function in type 1 diabetes. *N Engl J Med* 2020;382:2493–2503
4. Bjornstad P, Snell-Bergeon JK, Rewers M, et al. Early diabetic nephropathy: a complication of reduced insulin sensitivity in type 1 diabetes. *Diabetes Care* 2013;36:3678–3683
5. Soltoff SP. ATP and the regulation of renal cell function. *Annu Rev Physiol* 1986;48:9–31
6. Nangaku M. Chronic hypoxia and tubulointerstitial injury: a final common pathway to end-stage renal failure. *J Am Soc Nephrol* 2006;17:17–25
7. Singh DK, Winocour P, Farrington K. Mechanisms of disease: the hypoxic tubular hypothesis of diabetic nephropathy. *Nat Clin Pract Nephrol* 2008;4:216–226
8. Oh MS, Hwang G, Han S, et al. Sonographic growth charts for kidney length in normal Korean children: a prospective observational study. *J Korean Med Sci* 2016;31:1089–1093
9. Pruijm M, Milani B, Burnier M. Blood oxygenation level-dependent MRI to assess renal oxygenation in renal diseases: progresses and challenges. *Front Physiol* 2017;7:667
10. de Boer A, Hartevelde AA, Stemkens B, et al. Multiparametric renal MRI: an intrasubject test-retest repeatability study. *J Magn Reson Imaging*, 16 April 2020. Available from <https://doi.org/10.1002/jmri.27167>
11. Gaspari F, Perico N, Matalone M, et al. Precision of plasma clearance of iohexol for estimation of GFR in patients with renal disease. *J Am Soc Nephrol* 1998;9:310–313
12. Jødal L, Brøchner-Mortensen J. Reassessment of a classical single injection ⁵¹Cr-EDTA clearance method for determination of renal function in children and adults. Part I: analytically correct relationship between total and one-pool clearance. *Scand J Clin Lab Invest* 2009;69:305–313
13. Battilana C, Zhang HP, Olshen RA, Wexler L, Myers BD. PAH extraction and estimation of plasma flow in diseased human kidneys. *Am J Physiol* 1991;261:F726–F733
14. Delanaye P, Radermecker RP, Rorive M, Depas G, Krzesinski JM. Indexing glomerular filtration rate for body surface area in obese patients is misleading: concept and example. *Nephrol Dial Transplant* 2005;20:2024–2028
15. Cherney DZ, Kanbay M, Lovshin JA. Renal physiology of glucose handling and therapeutic implications. *Nephrol Dial Transplant* 2020;35(Suppl. 1):i3–i12
16. Cherney DZ, Perkins BA, Soleymanlou N, et al. Renal hemodynamic effect of sodium-glucose cotransporter 2 inhibition in patients with type 1 diabetes mellitus. *Circulation* 2014;129:587–597
17. RISE Consortium. Metabolic contrasts between youth and adults with impaired glucose tolerance or recently diagnosed type 2 diabetes: I. observations using the hyperglycemic clamp. *Diabetes Care* 2018;41:1696–1706
18. Rickels MR, Evans-Molina C, Bahnson HT, et al.; T1D Exchange β -Cell Function Study Group. High residual C-peptide likely contributes to glycemic control in type 1 diabetes. *J Clin Invest* 2020;130:1850–1862
19. Williams KV, Erbey JR, Becker D, Arslanian S, Orchard TJ. Can clinical factors estimate insulin resistance in type 1 diabetes? *Diabetes* 2000;49:626–632
20. Prasad PV, Thacker J, Li LP, et al. Multi-parametric evaluation of chronic kidney disease by MRI: a preliminary cross-sectional study. *PLoS One* 2015;10:e0139661
21. Epstein FH, Prasad P. Effects of furosemide on medullary oxygenation in younger and older subjects. *Kidney Int* 2000;57:2080–2083
22. Layton AT, Laghmani K, Vallon V, Edwards A. Solute transport and oxygen consumption along the nephrons: effects of Na⁺ transport inhibitors. *Am J Physiol Renal Physiol* 2016;311:F1217–F1229
23. Layton AT, Vallon V. Renal tubular solute transport and oxygen consumption: insights from computational models. *Curr Opin Nephrol Hypertens* 2018;27:384–389
24. Sears B, Perry M. The role of fatty acids in insulin resistance. *Lipids Health Dis* 2015;14:121
25. Murea M, Freedman BI, Parks JS, Antinozzi PA, Elbein SC, Ma L. Lipotoxicity in diabetic nephropathy: the potential role of fatty acid oxidation. *Clin J Am Soc Nephrol* 2010;5:2373–2379
26. Hinkle PC. P/O ratios of mitochondrial oxidative phosphorylation. *Biochim Biophys Acta* 2005;1706:1–11
27. Chen Y, Fry BC, Layton AT. Modeling glucose metabolism and lactate production in the kidney. *Math Biosci* 2017;289:116–129
28. Körner A, Eklöf AC, Celsi G, Aperia A. Increased renal metabolism in diabetes. Mechanism and functional implications. *Diabetes* 1994;43:629–633
29. Layton AT, Vallon V, Edwards A. A computational model for simulating solute transport and oxygen consumption along the nephrons. *Am J Physiol Renal Physiol* 2016;311:F1378–F1390
30. Hansell P, Welch WJ, Blantz RC, Palm F. Determinants of kidney oxygen consumption and their relationship to tissue oxygen tension in diabetes and hypertension. *Clin Exp Pharmacol Physiol* 2013;40:123–137
31. Luo F, Liao Y, Cui K, Tao Y. Noninvasive evaluation of renal oxygenation in children with chronic kidney disease using blood-oxygen-level-dependent magnetic resonance imaging. *Pediatr Radiol* 2020;50:848–854
32. Pruijm M, Mendichovszky IA, Liss P, et al. Renal blood oxygenation level-dependent magnetic resonance imaging to measure renal tissue oxygenation: a statement paper and systematic review. *Nephrol Dial Transplant* 2018;33(Suppl. 2):ii22–ii8
33. Milani B, Ansaloni A, Sousa-Guimaraes S, et al. Reduction of cortical oxygenation in chronic kidney disease: evidence obtained with a new analysis method of blood oxygenation level-dependent magnetic resonance imaging. *Nephrol Dial Transplant* 2017;32:2097–2105
34. Bjornstad P, Lovshin JA, Lytvyn Y, et al. Adiposity impacts intrarenal hemodynamic function in adults with long-standing type 1 diabetes with and without diabetic nephropathy: results from the Canadian Study of Longevity in Type 1 Diabetes. *Diabetes Care* 2018;41:831–839
35. Humphreys BD, Xu F, Sabbiseti V, et al. Chronic epithelial kidney injury molecule-1 expression causes murine kidney fibrosis. *J Clin Invest* 2013;123:4023–4035

36. Bjornstad P, Maahs DM, Cherney DZ, et al. Insulin sensitivity is an important determinant of renal health in adolescents with type 2 diabetes. *Diabetes Care* 2014;37:3033–3039
37. Bjornstad P, Nehus E, El Ghormli L, et al.; TODAY Study Group. Insulin sensitivity and diabetic kidney disease in children and adolescents with type 2 diabetes: an observational analysis of data from the TODAY Clinical Trial. *Am J Kidney Dis* 2018;71:65–74
38. Amiel SA, Sherwin RS, Simonson DC, Lauritano AA, Tamborlane WV. Impaired insulin action in puberty. A contributing factor to poor glycemic control in adolescents with diabetes. *N Engl J Med* 1986;315:215–219
39. Cree-Green M, Stuppy JJ, Thurston J, et al. Youth with type 1 diabetes have adipose, hepatic, and peripheral insulin resistance. *J Clin Endocrinol Metab* 2018;103:3647–3657
40. Krolewski AS, Niewczas MA, Skupien J, et al. Early progressive renal decline precedes the onset of microalbuminuria and its progression to macroalbuminuria. *Diabetes Care* 2014;37:226–234
41. Perkovic V, Jardine MJ, Neal B, et al.; CREDENCE Trial Investigators. Canagliflozin and renal outcomes in type 2 diabetes and nephropathy. *N Engl J Med* 2019;380:2295–2306
42. van Raalte DH, Bjornstad P, Persson F, et al. The impact of sotagliflozin on renal function, albuminuria, blood pressure, and hematocrit in adults with type 1 diabetes. *Diabetes Care* 2019;42:1921–1929
43. Layton AT. Optimizing SGLT inhibitor treatment for diabetes with chronic kidney diseases. *Biol Cybern* 2019;113:139–148
44. Merovci A, Solis-Herrera C, Daniele G, et al. Dapagliflozin improves muscle insulin sensitivity but enhances endogenous glucose production. *J Clin Invest* 2014;124:509–514
45. Takagi S, Li J, Takagaki Y, et al. Ipragliflozin improves mitochondrial abnormalities in renal tubules induced by a high-fat diet. *J Diabetes Investig* 2018;9:1025–1032
46. Kim JY, Tfayli H, Bacha F, et al. β -cell function, incretin response, and insulin sensitivity of glucose and fat metabolism in obese youth: relationship to OGTT-time-to-glucose-peak. *Pediatr Diabetes* 2020;21:18–27